Journal of Applied Pharmaceutical Science Vol. 14(11), pp 071-081, November, 2024
Available online at http://www.japsonline.com
DOI: 10.7324/JAPS.2024.188231
ISSN 2231-3354

Diterpene alcohol fraction of *Cyperus rotundus* Linn essential oil regulates Bcl-2 and Bax expression inducing apoptosis on HeLa *in vitro* and *in silico*

Susianti Susianti[1]*, Yanwirasti Yanwirasti[2], Eryati Darwin[3], Jamsari Jamsari[4], Arif Setiawansyah[5]

[1]Department of Histology, Faculty of Medicine, Universitas Lampung, Bandar Lampung, Indonesia.
[2]Department of Anatomy, Faculty of Medicine, Universitas Andalas, Padang, Indonesia.
[3]Department of Histology, Faculty of Medicine, Universitas Andalas, Padang, Indonesia.
[4]Faculty of Agriculture, Universitas Andalas, Padang, Indonesia.
[5]Akademi Farmasi Cendikia Farma Husada, Bandar Lampung, Indonesia.

ARTICLE HISTORY

Received on: 27/06/2024
Accepted on: 10/09/2024
Available Online: 20/10/2024

Key words:
Diterpene alcohol, Cyperus rotundus, Apoptosis, HeLa, Bcl-2, Bax.

ABSTRACT

Apoptosis, or programmed cell death, is a crucial mechanism in preventing cancer growth, and one of the targets is reducing the expression of the anti-apoptotic protein Bcl-2. This study aimed to evaluate the potential of fractions from nutsedge (*Cyperus rotundus*) essential oil in inducing apoptosis and inhibiting the progression of cervical cancer. The researchers investigated the apoptosis-inducing activity of these fractions against the HeLa cervical cancer cell line using *in vitro* and *in silico* approaches. The cytotoxic effects were assessed through an MTT assay on HeLa cells cultured in 96-well plates. Additionally, flow cytometry with Annexin/PI staining was employed to analyze the induction of apoptosis by the fractions. The immunocytochemical staining of cells was also implemented to assess Bax and Bcl-2 expressions. The biologically active compound in fractions was screened using a molecular docking approach to Bcl-2 co-crystalized structure and their pharmacokinetics and toxicity profile were assessed. The cytotoxic activity differed significantly from each fraction. The highest cytotoxicity was observed in fraction 1 (IC50: 8.307 + 0.186 mcg/ml), and the lowest cytotoxicity was observed in fraction 4 (IC50:>500 mcg/ml). Fraction 1 decreased the Bcl-2 expression and increased the Bax expression. Molecular docking screening revealed that 5-(7a-isopropenyl-4,5-dimethyl-octahydro-inden-4-yl)-3-methyl-pent-2-en-1-ol was predicted as the main contributor to apoptosis-inducing activity of fraction 1. The supplementation of fraction 1 induces cell apoptosis on HeLa cells, indicating the potential of this fraction of nutsedge essential oil for developing an anti-cervical cancer agent.

INTRODUCTION

Cervical cancer remains one of the leading causes of cancer-related deaths among women worldwide, with an estimated 604,000 new cases and 342,000 deaths reported in 2020 [1]. While advances in early detection and treatment have improved survival rates, the development of chemoresistance and severe side effects associated with conventional chemotherapeutic agents highlight the urgent need for alternative, more effective, and less toxic therapeutic approaches [2,3]. Natural products derived from medicinal plants have gained significant attention in recent years due to their potential anticancer properties and reduced toxicity profiles [4,5].

Aside from being a quite promising source of therapeutic drugs for various diseases, natural products are also an excellent source of chemotherapeutic agents [6]. Many research has been focused on natural products for the discovery and development of anti-cancer agents, one of which is the potential of *Cyperus rotundus* L. *C. rotundus*, commonly known

*Corresponding Author
Susianti Susianti, Department of Histology, Faculty of Medicine, Universitas Lampung, Bandar Lampung, Indonesia.
E-mail: susiantiglb @ yahoo.com

as purple nutsedge, is a perennial sedge widely distributed in tropical and subtropical regions [7]. The essential oil extracted from its tubers has been traditionally used in various folk medicine practices for its anti-inflammatory, antimicrobial, and antioxidant properties [8,9]. Recent studies have suggested that the *C. rotundus* essential oil possesses potent cytotoxic activity against various cancer cell lines, including breast, lung, and cervical cancer cells [10–16].

The anti-cancer and cytotoxic potential of *C. rotundus* is ascribed to its rich spectrum of chemical constituents, which are pivotal in its biological efficacy [17]. Several studies have underscored the presence of various active compounds in *C. rotundus*, including sesquiterpenes such as cyperotundone, isocyperotundone, and cyperusol A flavonoids like quercetin, myricetin, and kaemferol, and alkaloids such as rotundine A, rotundine B, and rotundine C [18–20]. However, its fractions and the underlying molecular mechanisms by which this fraction exerts its anticancer effects, particularly in cervical cancer, remain largely unexplored.

In this study, we investigated the anticancer potential of the diterpene alcohol fraction isolated from *C. rotundus* essential oil against HeLa cervical cancer cells *in vitro* and *in silico*. Specifically, we aimed to elucidate the molecular mechanisms underlying the apoptotic effects of this fraction by evaluating its impact on the expression of Bcl-2 and Bax proteins. Our findings contribute to the growing body of knowledge on the therapeutic potential of natural products in cancer treatment and provide insights into the development of novel, targeted approaches for cervical cancer management.

MATERIALS AND METHODS

Chemicals and reagents

All chemicals and reagents used in the present study were analytical grade. The chemicals used for fractionation were provided by Merck, Germany including ethyl acetate, ethanol, methanol, choloroform, and toluene. The HeLa cells were obtained from the parasitology laboratory, Faculty of Medicine, Gadjah Mada University, and the polyconal antibody rabbit anti-human bcl-2 and bax were obtained from Bioss. The reagents for cytotoxic and apoptosis studies were RPMI 1640 media (Gibco, USA), fetal bovine serum (FBS) (Sigma-Aldrich, Singapore), penicillin-streptomycin (Sigma-Aldrich, Singapore), fungison (Gibco, USA), bicarbonate sodium (Bratachem, Indonesia), HEPES (Sigma-Aldrich, Singapore), DMSO (Sigma-Aldrich, Singapore), aquabidest (Bratachem, Indonesia), yellow MTT (Sigma-Aldrich, Singapore), sodium dodecyl sulfate (SDS) (Bio-Rad, Indonesia), acridine orange (Bio-Rad, Indonesia), ethydium bromide (Bio-Rad, Indonesia), Phosphate buffer serum, tripsin EDTA (Gibco, USA), annexin-V fluos-Pi (Roche, Switzerland), biotinylated secondary antibody, streptadivin-HRP, diaminobenzydine tetrahydrochloride (DAB), and mayer hematoxyline (Dako, Denmark).

Sample collection, extraction, and fractionation

Cyperus rotundus was collected from wild areas surrounding Bandar Lampung City, Lampung Province, Indonesia. The samples were botanically identified by Dr. Yuliyanti, Laboratory of Botany, Department of Biology, Faculty of Mathematics and Natural Science, Lampung University. The collected *C. rotundus* were sorted from unnecessary components and cleaned in a free-flowing water chamber. More after, the *C. rotundus* were then air-dried in a room temperature for 7 days. Approximately 10 kg of air-dried purple nutsedge rhizome were distilled using water distillation in round bottom flasks for 4 hours. The $MgSO_{4}.{}_{7}H_{2}O$ was added to the obtained essential oil to remove the water content. 15 ml of essential oil was produced and stored in a dark and closed glass bottle. The essential oil was then fractionated by inserting 8 g of essential oil into a column chromatography loaded with 50 g of silica gel 60 and eluted with 1 L MeOH-$CHCl_3$ (3:97). The fractions were collected into each 10 mL fraction tube and analyzed using GC-MS.

In vitro cytotoxic activity

The cytotoxic test was assessed using an MTT (3-[4,5-dimethylthiazol-2-yl]-2,5 diphenyltetrazolium bromide) dye reduction assay, based on a method described by Mosmann [21] with minor modification. A 96-well microculture plate was used for the experiment. A HeLa cell suspension of 2×10^4 cells was dissolved in 100 µl culture medium (RPMI 1640) containing 0.5% FBS in each well of the plate. The cells were then starved for 24 hours in a 5% CO_2 incubator at 37°C. Following starvation, the media was removed and replaced with fresh media containing 10% FBS, and test solutions (fractions and doxorubicin) were administered in 8 serial doses (80; 40; 20; 10; 5; 2.5; 1.25; 0.625 µg/ml) with three replications. The cultures were then incubated, added MTT (10 µl each well in 100 µl of cell suspensions), and incubated for 4 hours more at 37°C in a 5% CO_2 incubator. The last process was done by adding 100 µl of SDS (sodium dodecyl sulfate) (10% in 0.01N HCl) to each well and further incubated overnight. The absorbance of each culture solution was measured at 596 nm using an ELISA reader. The cell viability was counted using the following formula as explained by Utami *et al.* [13]:

$$\textit{Cell viability}\ (\%) = \frac{(A\text{-}B)}{(C\text{-}B)} \times 100$$

where:

A = Average absorbance of media + cell + test material
B = Average media absorbance
C = Average absorbance of media + cell

Apoptosis test

The apoptosis test was employed using a method described by Susianti *et al.* [12]. The most active fraction (exhibiting the most potent cytotoxic activity/lowest IC_{50}) was used for the apoptosis test on HeLa cells. HeLa cells were inserted into a 6-well microplate. Each well was filled with 1×10^6 cells/well in 500 µl of media (FBS 0.5%). Microcultures were incubated in an incubator for 24 hours. Then, the media in the microculture is removed, replaced with media (10% FBS), and given the test material dd into three groups (control, ½ IC_{50}, IC_{50}). The microcultures were additionally incubated overnight.

Before the treatment of the sample, a flow cytometry reagent was prepared by mixing 100 µl of buffer, 2 µl of PI, and Annexin-V. One well requires 650 µl buffer, 12 µl PI, and 12 µl Annexin-V. Eppendorf was wrapped in aluminum foil, as the reagent is not light-resistant. The preparation of this reagent is carried out with gloves due to carcinogenic compounds.

After making the flow cytometry reagent, the next step is sample preparation. One conical was prepared for one type of treatment and was marked on each conical. Media was taken from the well with a 1 ml micropipette and transferred to the conicle. 1 ml of PBS was added to each well and then transferred into the conicle. Trypsin-EDTA 0.25% (200 µl/well) was added and incubated at 37°C for 5 minutes followed by the addition of 1 ml of RPMI media and monitored under a microscope. The culture medium in the wells was displaced into the conical and centrifuged at 600 rpm for 5 minutes. The media is removed by pouring and then washing each pellet with 500 µl of cold PBS by resuspension so that the pellets that settle below dissolve in PBS. The pellet was transferred into an Eppendorf and centrifuged at 2,000 rpm for 3 minutes. The media was discarded, Annexin V-PI (100 µl) and buffer (350 µl) were added and incubated at 25°C for 10 minutes. The solution was transferred to the flow tube. The cell suspension is ready to be injected into the flow cytometer, and then the data on the computer is ready to be read.

Immunocytochemical staining of Bcl-2 and Bax expression

The most active fraction was used to assess Bcl-2 and Bax expression on the HeLa cell. Immunocytochemical staining was implemented by culturing the cell in two 24-well microplates (for Bcl-2 and Bax, respectively) covered with coverslips. Each well was filled with 1×10^5 cells in 500 µl 0.5% FBS and incubated for 24 hours.

A glass micro slide was taken, coated with a coverslip, incubated at 25°C for 1 hour. The coverslip-coated slides were then fixated with methanol for 5 minutes and washed with aquadest for 5 minutes. The slides were dipped in peroxidase-blocking solution for 10 minutes and incubated in prediluted blocking serum for 10 minutes at room temperature. 50–100 µl primary antibody (1:100) was then applied and incubated at 4°C humidified freezer overnight, followed by washing in PBS. A 50–100 µl biotinylated secondary antibody was added and incubated at 25°C for 15 minutes.

Furthermore, the slides were washed with PBS and incubated in streptavidin-HRP for 10 minutes, followed by a wash with PBS, applied with 100 µl DAB, incubated for 5 minutes, and washed with free-flowing water for 5 minutes. Counterstained was undertaken using 50–100 µl Mayer hematoxylin, washed with free-flowing water, and incubated at 25°C for 30 minutes. The slides were then dipped in ethanol, adding a few drops of mounting medium Entellan. The slides were observed under the microscope at a magnification of 400x.

***In silico* molecular docking prediction**

Compounds found in fractions were subjected to molecular docking using Autodock 4.2 equipped with the Autodock Tool user interface (The Scripps Research Institute). The ligand preparation was initially performed before molecular docking by drawing their 2D structure using Chemdraw Ultra 12.0 and converting to 3D using Chem 3D Pro. The ligand structure was optimized by applying MM2 energy minimization and saved in PDB format. The Bcl-2 was pointed out as the target macromolecule, and the crystallographic structure was retrieved from the Protein Data Bank (rcsb.org) with PDB ID: 4IEH [22]. The macromolecule was prepared in Biovia Discovery Studio to remove water, ligands, and heteroatoms. For docking purposes, the crystallographic structure of Bcl-2 was further processed in Autodock by adding hydrogen atoms. On the other hand, the center node and a number of rotatable bonds were set to ligands. The docking process was implemented to Bcl-2 active site (*x*: 12.153, *y*: 25.794, *z*: 11.85) with an adjustment of gridbox size (50 × 50 × 50; spacing 0.375 Å). The flexible-rigit docking was carried out using 100 runs of Genetic Algorithm with default crossreff and mutation with an output of Lamarckian GA. The molecular docking was undertaken as many as three repetitions.

***In silico* pharmacokinetics and toxicological assessment**

The Pharmacokinetics profile and the toxicological properties were assessed using biosig online pkCSM tool [23]. The screening used the canonical smile of the molecules to be inputted on the web server. The assessment was subjected to adsorption, distribution, metabolism, excretion (ADME), and toxicity parameters.

Statistical analysis

Statistical analysis of the cytotoxic data was undertaken using GraphPad Prism version 9.5.1. The probit analysis was used to convert the cell viability in a dose-response curve to obtain the IC_{50}. The significance of the result was assessed using One-Way ANOVA followed by a Tukey's test.

RESULT AND DISCUSSION

Fractionation

The fractionation yielded four fractions of varying masses (0.967 g, 5.291 g, 0.832 g, and 0.237 g), whose chemical compositions were subsequently analyzed via GC-MS. The chromatographic profiles, illustrated in Figure 1, exhibited a marked diversity in both the number and relative abundance of constituent peaks, where each peak corresponds to a distinct chemical compound present within the fraction. Remarkably, fraction 1 displayed the highest degree of complexity, comprising 67 discernible peaks, followed by fractions 4, 3, and 2 with 60, 59, and 50 peaks, respectively. Despite sharing several compounds across all fractions, as elucidated in Table 1, the incomplete separation of certain constituents suggests that the fractionation process was suboptimal, potentially attributable to the inadequate mobile phase employed. Additionally, the incomplete separation phenomenon could also be affected by the inability of silica gel used as the stationary phase to effectively separate chemical compounds due to their similar physicochemical properties [24]. This inefficient resolution highlights the critical need for further optimization of the mobile phase composition as well as the stationary phase to enhance the

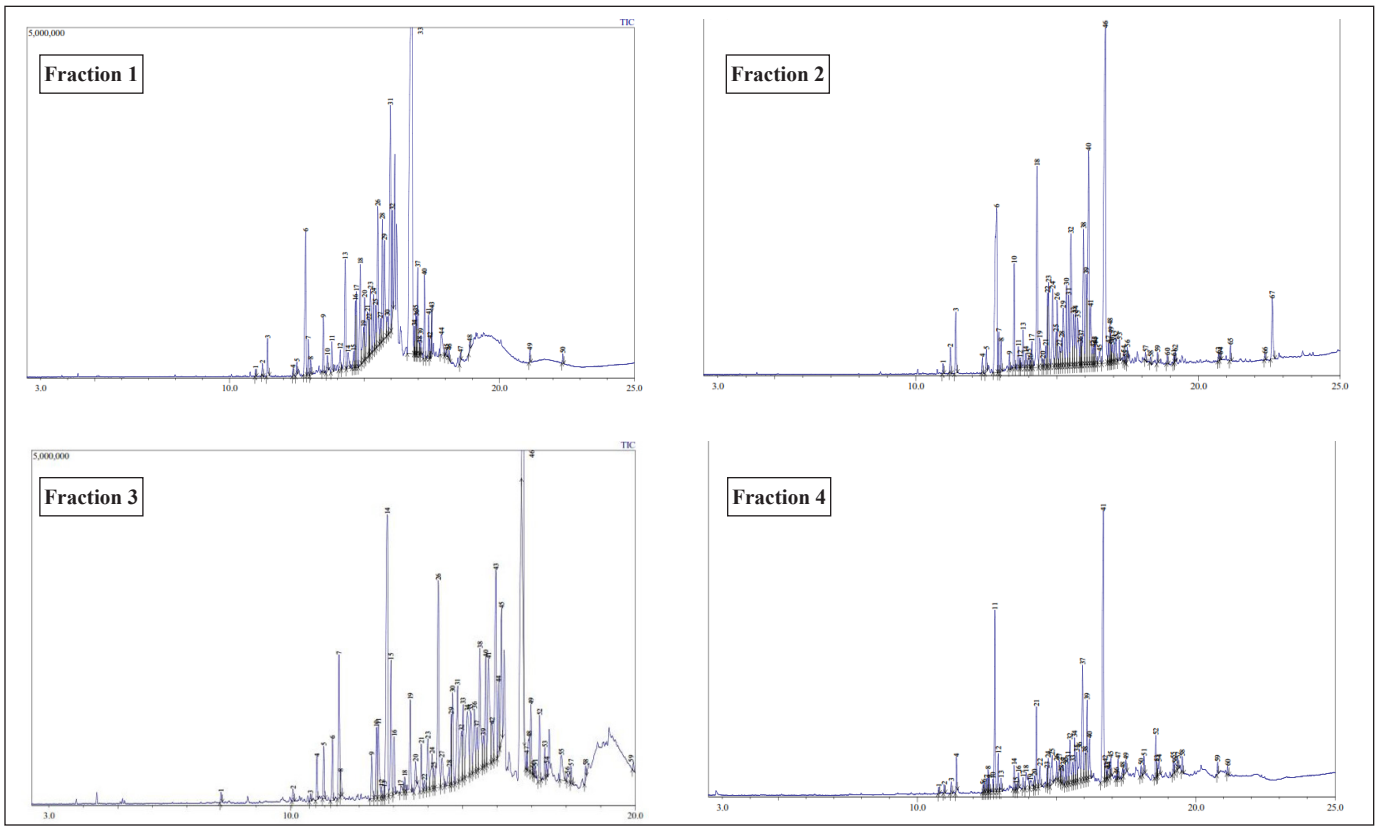

Figure 1. GC chromatogram of CrEO fractions.

Table 1. Chemical composition of CrEO fractions observed by GC-MS.

Compounds	Formula	Abundance (%)			
		Fraction 1	Fraction 2	Fraction 3	Fraction 4
Longiverbenone	C15H24O	17.55	31.58	6.27	20.64
β-selinene	C15H24	8.75	4.85	10.07	9.09
Caryophyllene oxide	C15H24O	6.23	3.78	6.42	3.90
5-(7a-isopropenyl-4,5-dimethyl-octahydro-inden-4-yl)-3-methyl-pent-2-en-1-ol	C20H34O	4.54	ND	ND	ND
2(3H)-naphthalenone	C15H22O	ND	7.97	5.81	7.02
1,6,6-trimethylhexahydro-1H-[1,3]dioxolo[4',5':4,5] cyclopenta[1,2-c]isoxazol-4-ol	C14H22N2	7.35	ND	ND	ND
4,4-dimethyl-3-ethyl-2-(2'-methyl-1'-propenyl)-2-cyclohexenone	C14H22O	ND	4.38	ND	ND
1,2-ethandiol	C2H6O2	ND	4.37	4.37	ND
1-cycloheptene	C15H24	ND	ND	ND	3.90

*ND = Not detected.

fractionation efficacy and achieve comprehensive separation of all components in subsequent isolation procedures.

Cytotoxic activity

The cytotoxic potential of the fractions was evaluated against HeLa cervical carcinoma cells, employing doxorubicin as a positive control, wherein cell viability and density served as indicators. The dose-response curves depicted in Figure 2 unequivocally demonstrate an inverse correlation between fraction concentration and cell viability, with higher doses eliciting more potent cytotoxicity across all fractions. Notably, the cytotoxic activity exhibited a marked divergence, with fraction 1 proving the most efficacious, followed by fractions 2, 3, and 4, as quantified in Table 2. This disparity

in cytotoxic potency is attributable to the distinct chemical compositions of each fraction, both in terms of the nature and relative abundance of constituent compounds. Fraction 1's superior cytotoxicity against HeLa cells can be ascribed to the presence of high levels of specific bioactive molecules, two of which were exclusive to this fraction. Additionally, fraction 2 displayed promising anti-proliferative effects, significantly outperforming the remaining fractions. However, it is noteworthy that while fractions 1 and 2 exhibited substantial cytotoxicity, their potency was inferior to the clinically employed chemotherapeutic agent doxorubicin. Nonetheless, these fractions warrant further investigation as prospective anticancer agents, given the well-established antineoplastic potential of numerous natural products documented extensively in the scientific literature.

Cyperus rotundus L. has garnered substantial scientific interest due to its remarkable cytotoxic potential across a diverse array of malignant cell lines, solidifying its medicinal value as a prospective chemotherapeutic agent. The hydro-methanolic extract derived from the stems of this species has exhibited a modest yet discernible apoptosis-inducing capability in K562 and L1210 leukemia cells. In a study, Sayed *et al.* [25] elucidated the cytotoxic propensities of steroid glycosides isolated from purple nutsedge stems against murine lymphoma cells (L5178Y). Corroborating these findings, Kilani *et al.* [26] unveiled that tuber extracts of *C. rotundus* exerted cytotoxic effects on L1210 leukemia cells by potentiating apoptosis. Intriguingly, comparative investigations have shed light on the differential cytotoxic potencies of chloroform and methanolic extracts against HeLa and SiHa cell lines, wherein the chloroform extract exhibited a pronounced superior efficacy, as reported by Susianti [27]. Remarkably, the ecological provenance of *C. rotundus* appears to modulate its cytotoxic capacity, as Utami *et al.* [13] elegantly delineated that specimens indigenous to highland regions exhibit an augmented potency against HeLa cells relative to their lowland and coastal counterparts. Furthermore, the essential oil distilled from purple nutsedge has also been demonstrated to exert cytotoxic effects on HeLa cells, as reported by Susianti *et al.* [12], further solidifying the auspicious therapeutic potential of this prodigious medicinal plant across its diverse specturm of phytochemical constituents.

Apoptosis assessment

In the quest to elucidate the apoptotic potential of the fractions, flow cytometric analysis coupled with the Annexin/PI assay was employed, wherein the most active fraction, identified as fraction 1 with the lowest IC_{50} value, was subjected to rigorous evaluation. An overview of the flow cytometric data obtained is presented in Figure 3. This technique provides a comprehensive visualization of living and deceased cells in the form of a quadrant-based diagram, with the R1 quadrant representing viable cells, R2 corresponding to early apoptosis, R3 depicting late apoptosis, and R4 indicating necrosis. Aligned with the objectives of this study, the percentages of cells occupying the R2 (early apoptosis) and R3 (late apoptosis)

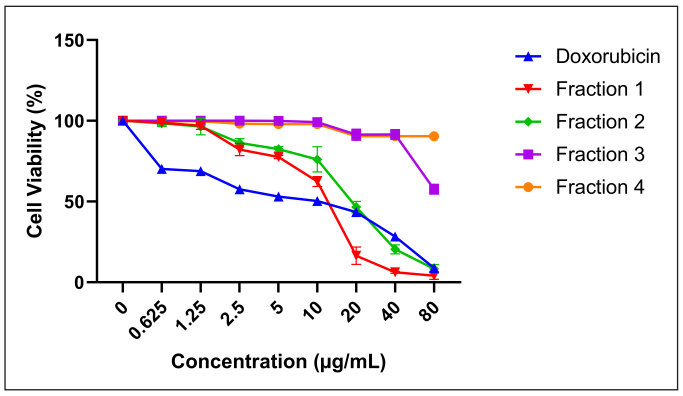

Figure 2. Effect of supplementation of CrEO fraction cell viability of the HeLa carcinoma cells.

Table 2. Cytotoxic activity of *C. rotundus* fractions on HeLa cells.

Samples	IC_{50} ± SD (µg/ml)
Fraction 1	8.307 ± 0.186[a]
Fraction 2	21.377 ± 9.543[a]
Fraction 3	>100[a]
Fraction 4	>100[a]
Doxorubicin	5.588 ± 0.490[a]

[a]*Treatments not sharing the same letters in the same row are significantly different by ANOVA followed by a Tukey's test ($p < 0.05$).*

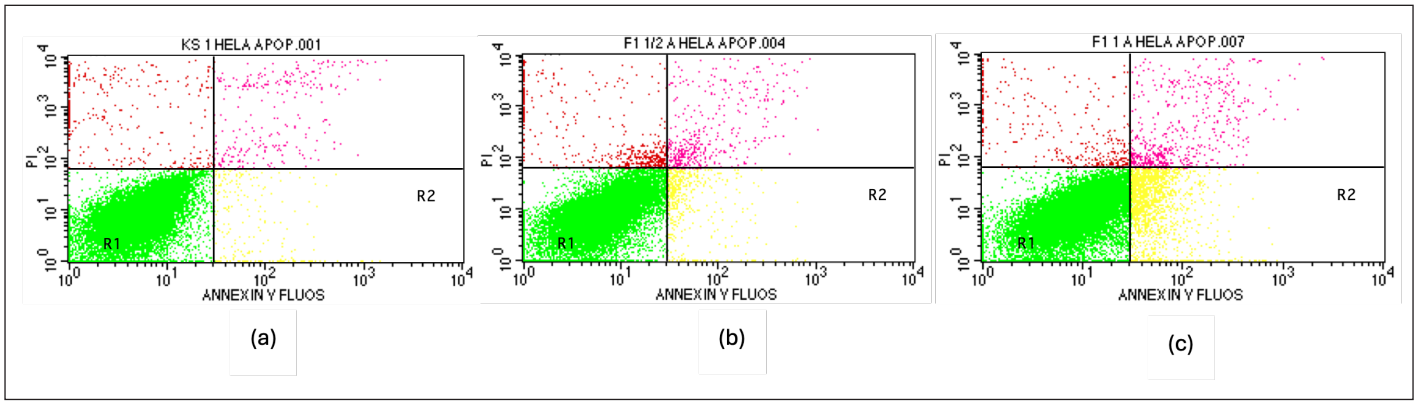

Figure 3. Apoptosis test result with flowcytometry method. (a) positive control, (b) fraction 1 at 4.154 µg/ml, and (c) fraction 1 at 8.307 µg/ml.

Table 3. Apoptosis activity of fraction 1.

Group	Cell apoptosis (%) ± SD
Control	2.383 ± 0.276[a]
½ IC_{50}	4.730 ± 0.200[a]
IC_{50}	11.153 ± 0.150[a]

[a]*Treatments not sharing the same letters in the same row are significantly different by ANOVA followed by a Tukey's test ($p < 0.05$).*

Table 4. The influence of supplementation of fraction 1 on Bax and Bcl-2 expression in HeLa cell.

Groups	Expression (%)	
	Bcl-2	Bax
Control	93.700 ± 6.29[a]	15.097 ± 5.89[b]
½ IC_{50}	64.094 ± 16.53[a]	27.571 ± 4.99[b]
IC_{50}	40.231 ± 19.61[a]	52.837 ± 11.90[b]

[a]*Treatments not sharing the same letters in the same row are significantly different by ANOVA followed by a Tukey's test ($p < 0.05$).*

quadrants were amalgamated to quantify the overall proportion of cells undergoing apoptosis. Remarkably, the data revealed a striking dose-dependent elevation in the frequency of apoptotic cells upon supplementation with fraction 1, as meticulously tabulated in Table 3. This profound correlation between fraction concentration and apoptotic induction underscores the profound cytotoxic potential of this active fraction, warranting further investigation into its therapeutic applications and mechanisms of action.

Bcl-2 and Bax expression

The supplementation of fraction 1 exerted a profound impact on the expression of the apoptotic regulators bcl-2 and bax in HeLa cells. Remarkably, a dose-dependent increase in bax expression was observed concomitantly with a decrease in bcl-2 levels, as elegantly depicted in Table 4. The anti-cancer mechanisms of action exhibited by natural products, particularly essential oils, are inherently diverse and intricate. Certain compounds can impede cellular proliferation and/or induce apoptosis by modulating the expression of proliferative genes or apoptosis regulators, culminating in cell cycle arrest [28]. Additionally, some constituents of essential oils exert anti-cancer effects by interfering with cell signaling and angiogenesis pathways [29]. In the present study, we unveil that fraction 1 of *C. rotundus* essential oil (CrEO) exhibits remarkable potential as an anti-cancer candidate by inducing apoptosis through the inhibition of Bcl-2 and concomitant upregulation of Bax expression, as vividly illustrated in Figure 4. These findings underscore the imperative for further elucidation of the molecular mechanisms underpinning the cytotoxic and therapeutic effects of this bioactive fraction.

Molecular docking prediction

To elucidate the bioactive compounds underpinning the cytotoxic and apoptosis-regulating effects of CrEO fractions,

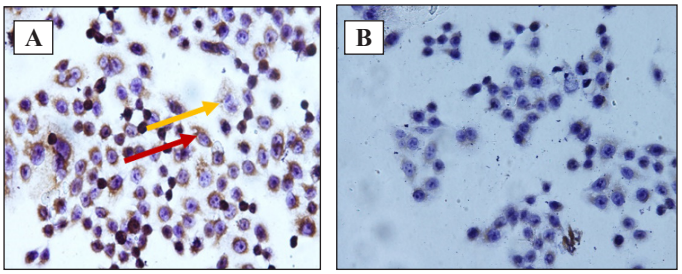

Figure 4. Immunocytochemical stained HeLa cell under the microscope (magnification 400x). A. Expression of Bax, B. Expression of Bcl-2. Note: red arrow indicated the cells express Bax/Bcl-2, yellow arrow indicated the cell does not express Bax/Bcl-2.

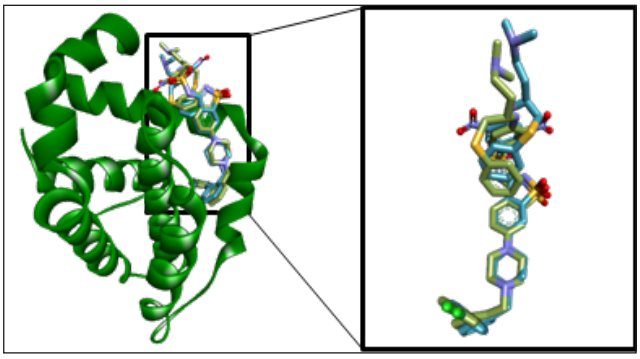

Figure 5. Superimposed of the best re-docking model to Bcl-2 with RMSD value of 1.559 Å (Original: green; Re-docked: blue)

Table 5. Docking score of CrEO fractions on Bcl-2.

Ligands	Docking score	
	ΔG (kcal/mol)	Ki (μM)
Longiverbenone	−6.49 ± 0.005	17.537 ± 0.009
β-selinene	−7.08 ± 0.008	6.41 ± 0.089
Caryophyllene oxide	−6.60 ± 0.017	14.52 ± 0.352
5-(7a-isopropenyl-4,5-dimethyl-octahydro-inden-4-yl)-3-methyl-pent-2-en-1-ol	−7.26 ± 0.064	4.79 ± 0.498
2(3H)-naphthalenone	−5.42 ± 0.005	107.00 ± 0.377
1,6,6-trimethylhexahydro-1H-[1,3]dioxolo[4',5':4,5] cyclopenta[1,2-c]isoxazol-4-ol	−4.77 ± 0.031	332.32 ± 1.127
4,4-dimethyl-3-ethyl-2-(2'-methyl-1'-propenyl)-2-cyclohexenone	−6.20 ± 0.01	28.52 ± 0.486
1,2-ethandiol	−2.25 ± 0.01	22174 ± 2.94
1-cycloheptene	−4.53 ± 0.005	474.19 ± 4.78
Native ligand	−14.52 ± 0.05	0.022 ± 0.002

a molecular docking approach was employed. Molecular docking simulations were performed against Bcl-2, considering the observed inhibition of Bcl-2 expression by CrEO fractions *in vitro*. To validate the docking protocol, a redocking simulation of the Bcl-2 native ligand was undertaken, wherein the docked pose was compared to the initial native ligand conformation. The accuracy of the protocol was substantiated by observing

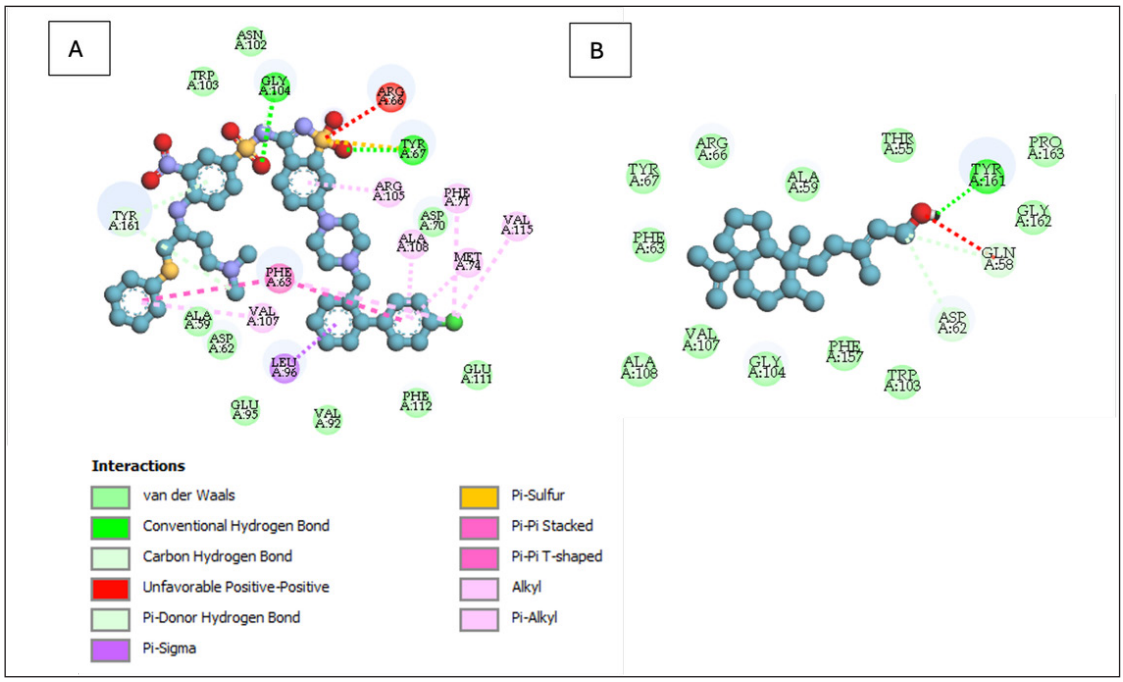

Figure 6. Molecular interactions of native ligand (A) and 5-(7a-isopropenyl-4,5-dimethyl-octahydro-inden-4-yl)-3-methyl-pent-2-en-1-ol (B) with Bcl-2.

Table 6. Adsorption profile of CrEO fractions.

Compounds	Caco-2	HIA (%)
Longiverbenone	1.171	87.467
β-selinene	1.429	95.574
Caryophyllene oxide	1.414	95.669
5-(7a-isopropenyl-4,5-dimethyl-octahydro-inden-4-yl)-3-methyl-pent-2-en-1-ol	1.525	95.215
2(3H)-naphthalenone	1.650	90.299
1,6,6-trimethylhexahydro-1H-[1,3] dioxolo[4',5':4,5]cyclopenta[1,2-c]isoxazol-4-ol	1.136	100
4,4-dimethyl-3-ethyl-2-(2'-methyl-1'-propenyl)-2-cyclohexenone	1.53	95.341
1,2-ethandiol	1.552	86.376
1-cycloheptene	1.374	96.014

the structural similarity between the docked pose and the native ligand, as depicted in Figure 5, with a root-mean-square deviation (RMSD) of 1.559 Å. An RMSD value below 2 Angstroms (Å) is generally considered adequate to validate a docking protocol effectively [30,31]. This benchmark indicates that the projected binding orientations closely resemble the experimental structures, considering the natural flexibility of proteins and the simplifications employed in docking algorithms [32].

A total of 9 major compounds identified across all fractions were subjected to molecular docking simulations against Bcl-2 to discern potential apoptosis inducers in HeLa cells. Table 5 reveals that 5-(7a-isopropenyl-4,5-dimethyl-octahydro-inden-4-yl)-3-methyl-pent-2-en-1-ol exhibited the most promising docking score among the evaluated compounds, albeit not surpassing the affinity of the native ligand. The potent cytotoxic activity of fraction 1 was hypothesized to stem from the presence of this compound, which was absent in the other fractions. The conformation adopted by 5-(7a-isopropenyl-4,5-dimethyl-octahydro-inden-4-yl)-3-methyl-pent-2-en-1-ol within the Bcl-2 active site renders it more conducive to interact with essential amino acid residues. Figure 6 illustrates the differential interactions between 5-(7a-isopropenyl-4,5-dimethyl-octahydro-inden-4-yl)-3-methyl-pent-2-en-1-ol and the native ligand with crucial amino acid residues of Bcl-2. The types of amino acids, interactions, and their respective numbers vary substantially, leading to distinct binding strengths to Bcl-2, thereby potentially accounting for the observed cytotoxic effects [33,34].

In silico pharmacokinetics and toxicological assessment

The comprehensive evaluation of the pharmacokinetic and toxicological profiles of the identified chemical constituents in CrEO fractions was conducted to ascertain their suitability for therapeutic development. The ADME parameters, and toxicity assessments were interpreted according to the guidelines established by Pires *et al.* [23]. Considering the prospective oral administration route, the initial parameter scrutinized was the absorption profile of the molecules. Several indices, including human intestinal absorption (HIA) and Caco-2 permeability, were employed to gauge the absorption potential. As depicted in Table 6, all identified compounds exhibited excellent absorption profiles, characterized by HIA values exceeding 80% and Caco-2 values greater than 0.90, indicating favorable intestinal permeability, as per the criteria proposed by Pérez *et al.* [35].

The distribution profile screening (Table 7) unveiled that most compounds identified in CrEO fractions exhibited a high volume of distributions (VD > 0.45 log l/kg), indicative

Table 7. Distribution profile of CrEO fractions.

Compounds	VDss (log L/Kg)	BBB permeability (log BB)	CNS Permeability (log PS)	Fraction Unbound (Fu)
Longiverbenone	0.619	0.661	−2.52	0.312
β-selinene	0.639	0.816	−1.461	0.089
Caryophyllene oxide	0.564	0.647	−2.521	0.327
5-(7a-isopropenyl-4,5-dimethyl-octahydro-inden-4-yl)-3-methyl-pent-2-en-1-ol	0.468	0.73	−1.772	0
2(3H)-naphthalenone	0.234	0.086	−1.98	0.443
1,6,6-trimethylhexahydro-1H-[1,3]dioxolo[4',5':4,5] cyclopenta[1,2-c]isoxazol-4-ol	0.178	−0.186	−3.032	0.683
4,4-dimethyl-3-ethyl-2-(2'-methyl-1'-propenyl)-2-cyclohexenone	0.351	0.6	−2.2	0.311
1,2-ethandiol	−0.359	−0.319	−2.916	0.849
1-cycloheptene	0.298	0.323	−2.69	0.621

Table 8. Metabolism profile of CrEO fractions.

Compounds	CYP2D6 substrate	CYP3A4 substrate	CYP1A2 inhibitor	CYP2C19 inhibitor	CYP2C9 inhibitor	CYP2D6 inhibitor	CYP3A4 inhibitor
Longiverbenone	No	No	No	No	No	No	No
β-selinene	No	Yes	Yes	No	No	No	No
Caryophyllene oxide	No	No	Yes	Yes	Yes	No	No
5-(7a-isopropenyl-4,5-dimethyl-octahydro-inden-4-yl)-3-methyl-pent-2-en-1-ol	No	Yes	Yes	No	No	No	No
2(3H)-naphthalenone	No	No	No	No	No	No	No
1,6,6-trimethylhexahydro-1H-[1,3] dioxolo[4',5':4,5]cyclopenta[1,2-c]isoxazol-4-ol	No	No	No	No	No	No	No
4,4-dimethyl-3-ethyl-2-(2'-methyl-1'-propenyl)-2-cyclohexenone	No	No	No	No	No	No	No
1,2-ethandiol	No	No	No	No	No	No	No
1-cycloheptene	No	No	No	No	No	No	No

Table 9. Excretion profile of CrEO fractions.

Compounds	Total clearance (ml/minute/kg)	Renal OCT2 substrate
Longiverbenone	7.21107479	No
β-selinene	14.9279441	No
Caryophyllene oxide	8.03526122	No
5-(7a-isopropenyl-4,5-dimethyl-octahydro-inden-4-yl)-3-methyl-pent-2-en-1-ol	19.9526231	No
2(3H)-naphthalenone	1.69044093	No
1,6,6-trimethylhexahydro-1H-[1,3] dioxolo[4',5':4,5]cyclopenta[1,2-c] isoxazol-4-ol	15.2405275	No
4,4-dimethyl-3-ethyl-2-(2'-methyl-1'-propenyl)-2-cyclohexenone	20.7014134	No
1,2-ethandiol	4.21696503	No
1-cycloheptene	1.60694125	No

Table 10. Toxicity profile of CrEO fractions.

Compounds	AMES toxicity	Hepatotoxicity
Longiverbenone	No	No
β-selinene	Yes	No
Caryophyllene oxide	No	No
5-(7a-isopropenyl-4,5-dimethyl-octahydro-inden-4-yl)-3-methyl-pent-2-en-1-ol	No	No
2(3H)-naphthalenone	No	Yes
1,6,6-trimethylhexahydro-1H-[1,3] dioxolo[4',5':4,5]cyclopenta[1,2-c] isoxazol-4-ol	No	No
4,4-dimethyl-3-ethyl-2-(2'-methyl-1'-propenyl)-2-cyclohexenone	No	No
1,2-ethandiol	No	No
1-cycloheptene	No	No

of substantial tissue distribution. However, a few compounds, such as 2(3H)-naphthalenone, 1,6,6-trimethylhexahydro-1H-[1,3]dioxolo[4',5':4,5]cyclopenta[1,2-c]isoxazol-4-ol, and 1-cycloheptene, demonstrated moderate (−0.15 – 0.45 log l/kg) or low (< −0.15 log l/kg) VD values. The volume of distribution reflects the extent to which a molecule is distributed across tissues or confined to the plasma compartment. Furthermore, all compounds exhibited high plasma protein binding, as evidenced by their low free fraction (Fu) values, potentially influencing their pharmacodynamic profiles. Remarkably, most CrEO compounds were predicted to cross the blood–brain barrier (BBB) (log BB > 0.3). However, despite this ability, not all compounds readily penetrated the central nervous system (CNS), as indicated by their log PS values (Table 6), with only β-selinene and 2(3H)-naphthalene exhibiting favorable CNS permeability (log PS > −0.2).

The metabolism profile of CrEO fractions was assessed by evaluating their potential to inhibit or act as substrates for CYP450 enzymes, which play a pivotal role in drug metabolism. Inhibition or induction of these enzymes can significantly influence the toxicity and therapeutic effects of a molecule [36,37]. As described in Table 8, among all compounds, only β-selinene and caryophyllene oxide interacted with CYP450 isoforms. Specifically, β-selinene acted as a CYP3A4 substrate and a CYP1A2 inhibitor, while caryophyllene oxide inhibited CYP1A2, CYP2C19, and CYP2C9.

The excretion profile was evaluated by assessing the total clearance and the compounds' interactions with the renal organic cation transporter 2 (OCT2), either as substrates or non-substrates. Total clearance and OCT2 interactions are crucial factors influencing a molecule's bioavailability, half-life, and subsequent dosing regimens [38]. Table 9 describes all identified compounds in CrEO fractions that have total clearance > 1 ml/minute/kg. Paine *et al.* [39] divided the total clearance of a molecule into three categories, including high (CLtot > 1 ml/minute/kg), medium (CLtot > 0.1 ml/minute/kg to < 1 ml/minute/kg), and low (CLtot ≤ 0.1). Thus, all compounds can be specified to have high total clearance. Additionally, none of the compounds act as renal OCT2 substrate, diminishing the risk of their interaction when consumed with other molecules that act as OCT2 inhibitors [40].

The toxicological assessment encompassed evaluations of mutagenicity (AMES toxicity) and hepatotoxicity to ascertain the safety profiles of the identified compounds in CrEO fractions. Table 10 revealed that several components, such as β-selinene and 2(3H)-naphthalenone, exhibited poor toxicity profiles by inducing mutagenicity and hepatotoxicity, while most compounds displayed excellent toxicity profiles.

The comprehensive pharmacokinetic and toxicological profiles of the identified compounds in CrEO fractions provide a rational basis for further development. Notably, 5-(7a-isopropenyl-4,5-dimethyl-octahydro-inden-4-yl)-3-methyl-pent-2-en-1-ol emerged as the most promising candidate, exhibiting excellent pharmacokinetic and toxicity properties, coupled with its potential to inhibit Bcl-2 expression by stably binding to the Bcl-2 active site and interacting with several essential amino acid residues. These findings underscore the compelling prospect of developing 5-(7a-isopropenyl-4,5-dimethyl-octahydro-inden-4-yl)-3-methyl-pent-2-en-1-ol as a novel anti-cancer agent, particularly for cervical cancer.

CONCLUSION

In conclusion, this study unveiled the remarkable cytotoxic potential of the diterpene alcohol fractions derived from CrEO against HeLa cervical cancer cells. Notably, fractions 1 and 2 exhibited potent cytotoxicity, with fraction 1 emerging as the most active. Mechanistic investigations revealed that fraction 1 potentiated apoptosis in HeLa cells by upregulating the pro-apoptotic protein Bax while concomitantly inhibiting the anti-apoptotic Bcl-2 protein. Molecular docking simulations and pharmacokinetic evaluations identified 5-(7a-isopropenyl-4,5-dimethyl-octahydro-inden-4-yl)-3-methyl-pent-2-en-1-ol as the key bioactive constituent underpinning the cytotoxic and apoptosis-inducing activities of fraction 1. This compound exhibited stable binding to the Bcl-2 active site, interacting with crucial amino acid residues implicated in modulating apoptosis. Moreover, 5-(7a-isopropenyl-4,5-dimethyl-octahydro-inden-4-yl)-3-methyl-pent-2-en-1-ol displayed favorable pharmacokinetic properties, including excellent absorption, distribution, metabolism, and excretion profiles, coupled with a desirable toxicity profile. Collectively, these findings accentuate the therapeutic potential of the diterpene alcohol fractions, particularly fraction 1, as a novel anticancer agent targeting cervical cancer. The identification of 5-(7a-isopropenyl-4,5-dimethyl-octahydro-inden-4-yl)-3-methyl-pent-2-en-1-ol as the primary bioactive constituent offers a promising lead for the development of targeted therapies against cervical malignancies by modulating the intrinsic apoptotic pathway.

AUTHOR CONTRIBUTIONS

All authors made substantial contributions to conception and design, acquisition of data, or analysis and interpretation of data; took part in drafting the article or revising it critically for important intellectual content; agreed to submit to the current journal; gave final approval of the version to be published; and agree to be accountable for all aspects of the work. All the authors are eligible to be an author as per the International Committee of Medical Journal Editors (ICMJE) requirements/guidelines.

FINANCIAL SUPPORT

There is no funding to report.

CONFLICTS OF INTEREST

The authors report no financial or any other conflicts of interest in this work.

ETHICAL APPROVALS

This study does not involve experiments on animals or human subjects.

DATA AVAILABILITY

All data generated and analyzed are included in this research article.

PUBLISHER'S NOTE

All claims expressed in this article are solely those of the authors and do not necessarily represent those of the publisher, the editors and the reviewers. This journal remains neutral with regard to jurisdictional claims in published institutional affiliation.

USE OF ARTIFICIAL INTELLIGENCE (AI)-ASSISTED TECHNOLOGY

The authors declares that they have not used artificial intelligence (AI)-tools for writing and editing of the manuscript, and no images were manipulated using AI.

REFERENCES

1. Sung H, Ferlay J, Siegel RL, Laversanne M, Soerjomataram I, Jemal A, *et al.* Global Cancer Statistics 2020: GLOBOCAN Estimates of incidence and mortality Worldwide for 36 Cancers in 185 Countries. CA Cancer J Clin. 2021;71(3):209–49. Available from: https://acsjournals.onlinelibrary.wiley.com/doi/abs/10.3322/caac.21660
2. Singh N, Kumar A. Insights into Ovarian Cancer: chemo-diversity, dose depended toxicities and survival responses. Med Oncol. 2023;40(4):111. Available from: https://doi.org/10.1007/s12032-023-01976-0
3. Jasrotia R, Dhanjal DS, Bhardwaj S, Sharma P, Chopra C, Singh R, *et al.* Nanotechnology based vaccines: cervical cancer management and perspectives. J Drug Deliv Sci Technol. 2022;71:103351. Available from: https://www.sciencedirect.com/science/article/pii/S1773224722002611
4. Newman DJ, Cragg GM. Natural products as sources of new drugs over the nearly four decades from 01/1981 to 09/2019. J Nat Prod. 2020 Mar 27;83(3):770–803. Available from: https://doi.org/10.1021/acs.jnatprod.9b01285
5. Farnsworth NR. Screening plants for new medicine. In: Staff S, Wilson E, editors. Biodiversity. Washington, DC: National Academy of Sciences Press; 1988. p. 83–97.
6. Cragg GM, Newman DJ. Plants as a source of anti-cancer agents. J Ethnopharmacol. 2005;100(1):72–9.
7. Kamala A, Middha SK, Karigar CS. Plants in traditional medicine with special reference to *Cyperus rotundus* L.: a eeview. 3 Biotech. 2018;8(3):309.
8. Essaidi I, Koubaier HBH, Snoussi A, Casabianca H, Chaabouni MM, Bouzouita N. Chemical composition of *Cyperus rotundus* L. tubers essential oil from the South of Tunisia, antioxidant potentiality and antibacterial activity against foodborne pathogens. J Essent Oil-Bearing Plants. 2014;17(3):522–32.
9. Rajamanickam M, Rajamanickam A. Analgesic and anti-inflammatory activity of the extracts from *Cyperus rotundus* Linn Rhizomes. J Appl Pharm Sci. 2016;6(9):197–203.
10. Singh N, Pandey BR, Verma P, Bhalla M, Gilca M. Phyto-pharmacotherapeutics of *Cyperus rotundus* Linn. (Motha): an overview. Indian J Nat Prod Resour. 2012;3(4):467–76.
11. Sivapalan SR. Medicinal uses and pharmacological activities of *Cyperus rotundus* Linn—a review. Int J Sci Res Public. 2013;3(1):2250–3153.
12. Susianti S, Yanwirasti Y, Darwin E, Jamsari. The cytotoxic effects of purpel nutsedge (*Cyperus rotundus* L.) tuber essential oil on the hela cervical cancer cell line. Paksitan J Biotech. 2016;15(2):1–23.
13. Utami N, Susianti S, Bakri S, Kurniawan B, Setiawansyah A. Cytotoxic activity of *Cyperus rotundus* L. Rhizome collected from three ecological zones in Lampung-Indonesia Against HeLa Cervical Cancer Cell. J Appl Pharm Sci. 2023;13(10):141–8. 14. Simorangkir D, Masfria M, Harahap U, Satria D. Activity anticancer N-hexane fraction of *Cyperus rotundus* L. Rhizome to breast cancer MCF-7 cell l;ine. Open Access Maced J Med Sci. 2019;7(22):3904–6.
15. Mannarreddy P, Denis M, Munireddy D, Pandurangan R, Thangavelu KP, Venkatesan K. Cytotoxic effect of *Cyperus rotundus* Rhizome extract on human cancer cell lines. Biomed Pharmacother. 2017;95:1375–87.
16. Memariani T, Hosseini T, Kamali H, Mohammadi A, Ghorbani M, Shakeri A, *et al.* Evaluation of the cytotoxic effects of *Cyperus longus* extract, fractions and its essential oil on the PC3 and MCF7 cancer cell lines. Oncol Lett. 2016;11(2):1353–60.
17. Hu QP, Cao XM, Hao DL, Zhang LL. Chemical composition, antioxidant, DNA damage protective, cytotoxic and antibacterial activities of *Cyperus rotundus* Rhizomes essential oil against foodborne pathogens. Sci Rep. 2017;7(December 2016):1–9.
18. Wang Q, Yi C, Duan W, Duan Y, Lou J, Zeng G, *et al.* Two new sesquiterpenoids isolated from *Cyperus rotundus* L. Nat Prod Commun. 2021;16(2):1934578X2199168.
19. Jeong SJ, Miyamoto T, Inagaki M, Kim YC, Higuchi R. Rotundines A−C, Three novel Sesquiterpene Alkaloids from Cyperus rotundus. J Nat Prod. 2000;63(5):673–5. https://doi.org/10.1021/np990588r
20. Samariya K, Sarin R. Isolation and identification of flavonoids from *Cyperus rotundus* Linn. *in vivo* and *in vitro*. J Drug Deliv Therap. 2013;3(2):109–13.
21. Mosmann T. Rapid colorimetric assay for cellular growth and survival: application to proliferation and cytotoxicity assays. J Immunol Methods. 1983;65(1–2):55–63.
22. Touré BB, Miller-Moslin K, Yusuff N, Perez L, Doré M, Joud C, *et al.* The role of the acidity of N-Heteroaryl sulfonamides as inhibitors of Bcl-2 family protein–protein interactions. ACS Med Chem Lett. 2013;4(2):186–90. https://doi.org/10.1021/ml300321d
23. Pires DE, Blundell TL, Ascher DB. pkCSM: predicting small-molecule pharmacokinetic properties using graph-based signatures (Theory-How to Enterpret pkCSM Result). pKCSM. 2015;58(9):4066–72. Available from: http://biosig.unimelb.edu.au/pkcsm/theory
24. Setiawansyah A, Arsul MI, Sukrasno S, Damayanti S, Insanu M, Fidrianny I. Anti-hyperuricemic potential of caryophyllene from *Syzygium aromaticum* essential oil: SiO_2-$AgNO_3$-based column chromatography purification, antioxidant, and Xanthine Oxidase inhibitory activities. Adv Trad Med. 2024;24:475–87. https://doi.org/10.1007/s13596-023-00710-5
25. Sayed HM, Mohamed MH, Farag SF, Mohamed GA, Proksch P. A new steroid glycoside and furochromones from *Cyperus rotundus* L. Nat Prod Res. 2007 Apr;21(4):343–50.
26. Kilani S, Ledauphin J, Bouhlel I, Ben Sghaier M, Boubaker J, Skandrani I, *et al.* Comparative study of *Cyperus rotundus* essential oil by a modified GC/MS analysis method. Evaluation of its antioxidant, cytotoxic, and apoptotic effects. Chem Biodivers. 2008;5(5):729–42.
27. Susianti S. Selektivitas Ekstrak Umbi Rumput Teki (*Cyperus rotundus* L.) Terhadap Sel HeLa dan SiHa Serta Pengaruhnya Terhadap Apoptosis. Yogyakarta, Indonesia: Universitas Gadjah Mada; 2009.
28. Gautam N, Mantha AK, Mittal S. Essential oils and their constituents as anticancer agents: a mechanistic view. BioMed Res Int. 2014;24:154106–29.
29. Mohamed Abdoul-Latif F, Ainane A, Houmed Aboubaker I, Mohamed J, Ainane T. Exploring the potent anticancer activity of essential oils and their bioactive compounds: mechanisms and prospects for future cancer therapy. Pharmaceuticals. 2023;16(8):1086–112.
30. Huang SY, Grinter SZ, Zou X. Scoring functions and their evaluation methods for protein–ligand docking recent advances and future directions. Phys Chem Chem Phys. 2010;12(40):12899–908. http://dx.doi.org/10.1039/C0CP00151A
31. Mukherjee S, Balius TE, Rizzo RC. Docking validation resources: protein family and ligand flexibility experiments. J Chem Inf Model. 2010;50(11):1986–2000.

32. Setiawansyah A, Reynaldi MA, Tjahjono DH, Sukrasno S. Molecular docking-based virtual screening of antidiabetic agents from Songga (*Strychnos lucida* R.Br.): an Indonesian Native Plant. Curr Res Biosci Biotech. 2022;3(2):208–14.
33. Reynaldi MA, Setiawansyah A. Potensi anti-Kanker Payudara Tanaman Songga (*Strychnos lucida* R. Br): Tinjauan Interaksi Molekuler Terhadap Reseptor Estrogen-α *In Silico*. Sasambo J Pharm. 2022;3(1):30–5.
34. Setiawansyah A, Arsul MI, Adliani N, Wismayani L. HMG-CoA reductase inhibitory activity potential of Iota-, Kappa-, and Lambda-carrageenan: a molecular docking approach. Ad-Dawaa' J Pharm Sci. 2022;5(2):94–102.
35. Pérez MAC, Sanz MB, Torres LR, Avalos RG, González MP, Díaz HG. A topological sub-structural approach for predicting human intestinal absorption of drugs. Eur J Med Chem. 2004;39(11):905–16.
36. Issa NT, Wathieu H, Ojo A, Byers SW, Dakshanamurthy S. Drug metabolism in preclinical drug development: a survey of the discovery process, toxicology, and computational tools. Curr Drug Metab. 2017;18(6):556–65.
37. Durán-Iturbide NA, Díaz-Eufracio BI, Medina-Franco JL. *In Silico* ADME/Tox profiling of natural products: a focus on BIOFACQUIM. ACS Omega. 2020;5(26):16076–84.
38. Doogue MP, Polasek TM. Drug dosing in renal disease. Clin Biochem Rev. 2011;32(2):69–73.
39. Paine SW, Ménochet K, Denton R, McGinnity DF, Riley RJ. Prediction of human renal clearance from preclinical species for a diverse set of drugs that exhibit both active secretion and net reabsorption. Drug Metab Dispos. 2011 Jun;39(6):1008–13.
40. Hacker K, Maas R, Kornhuber J, Fromm MF, Zolk O. Substrate-dependent inhibition of the human organic cation transporter OCT2: a comparison of metformin with experimental substrates. PLoS One. 2015;10(9):e0136451.

How to cite this article:
Susianti S, Yanwirasti Y, Darwin E, Jamsari J, Setiawansyah A. Diterpene alcohol fraction of *Cyperus rotundus* Linn essential oil regulates Bcl-2 and Bax expression inducing apoptosis on HeLa *in vitro* and *in silico*. J Appl Pharm Sci. 2024;14(11):071–081.